

Effect of solution molarity on properties of hydrothermally grown ZnO nanostructures

Yi Chen¹, Wei-You Chen¹, Hung-Pin Hsu¹, Jiunn-Chyi Lee² and Ya-Fen Wu^{1,3*}

¹Department of Electronic Engineering, Ming Chi University of Technology, New Taipei City 243, Taiwan

²Department of Electrical Engineering, Taipei City University of Science and Technology, Taipei 112, Taiwan

³College of Engineering, Chang Gung University, Taoyuan 333, Taiwan

Email: yfwu@mail.mcut.edu.tw

Abstract. In this work, the hydrothermally grown ZnO nanostructures were successfully prepared on indium tin oxide glass using different aqueous solution molarities. The effect of solution molarity on the structural and optical properties of ZnO nanostructures were studied by X-ray diffraction and temperature-dependent photoluminescence (PL) measurements. The PL intensity ratio of the ultraviolet emission to the visible emission is also calculated. It is found that the crystal quality and the optical properties are improved by raising the solution molarity, but too higher solution molarity should lead to the disorder of ZnO structures, and deteriorate the crystal quality.

1. Introduction

Zinc oxide (ZnO) has been extensively investigated due to its unique properties, including wide direct bandgap energy (3.36 eV), large exciton binding energy (60 meV), high piezoelectricity, high electron mobility, and thermal stability. These characteristics make ZnO nanostructures interesting for application in ultraviolet (UV) light emitters, optoelectronic devices, and chemical sensors as well as acousto-optic, electro-optic, and piezoelectric material [1-3]. ZnO nanostructures with small dimensions exhibit distinctive properties arising from their nanoscale size and shapes. The roles of the nanostructure size, impurities, and morphology are very important to their applications. ZnO nanostructures have been synthesized by different methods, including metal-organic chemical vapor deposition (MOCVD) [4], physical vapor phase deposition [5], and the low temperature hydrothermal method [6]. The hydrothermal method, which involves heterogeneous nucleation in super saturated solutions for the growth of nanostructures on the surface, has been widely used to ZnO structures on ZnO-seeded substrate. The advantages of this method include low-cost, low-temperature, nanoelectronic compatible, and suitable for large area substrates. The properties of ZnO produced by the hydrothermal method are dependent upon preparation parameters such as growth temperature, solution molarity, and deposition time [7]. In this work, the hydrothermally grown ZnO nanostructures were prepared with different aqueous solution molarities. Measurements of X-ray diffraction (XRD) and temperature dependent photoluminescence (PL) were performed to examine the structural and optical properties of the ZnO nanostructures.



2. Experimental

A thin film of zinc acetate (comprised of a solution containing zinc acetate dihydrate $\text{Zn}(\text{CH}_3\text{COO})_2 \cdot 2\text{H}_2\text{O}$) was spin coated onto an indium-tin-oxide (ITO) glass substrate and annealed at $300\text{ }^\circ\text{C}$ in oxygen for 20 min. The hydrothermal method was used to grow ZnO nanostructures on ITO glass using an aqueous solution of zinc nitrate dehydrate ($\text{Zn}(\text{NO}_3)_2$) and hexamethylenetetramine (HMTA) which were dissolved in 100 ml of deionized (DI) water. The molarities of solutions were set to 10, 20, 30, 40, and 50 mM and the growth temperatures were set to $90\text{ }^\circ\text{C}$. The growth was carried out for 3 hours after the temperature of the aqueous solution reached $90\text{ }^\circ\text{C}$. Finally, the sample was taken out from the aqueous solution and immersed into DI water to remove any residue on the substrate. After growth, the samples were characterized by HRXRD. Rocking curves of the (002) reflection were produced using the Bede D1 system. The temperature dependent PL measurements were carried out by mounting the sample in a closed cycle helium cryostat where the temperature (T) was varied from 10 to 300 K and using a He-Cd laser operating at a wavelength of 325 nm and the average excitation intensity was 30 mW. The luminescence signal was dispersed through a 0.5 m monochromator and detected using a silicon photodiode by standard lock-in amplification technique.

3. Results and discussion

Figure 1 shows the XRD patterns of the ZnO nanostructures with the solution molarities from 10 to 50 mM. The nanocrystalline quality could be analyzed using XRD measurements. It can be seen that the detected diffraction peaks from the nanocrystallite responses have a wurtzite hexagonal ZnO structure and the narrow broadenings indicate good crystallinity of the as-synthesized products. The distinct diffraction of the ZnO can be indexed as corresponding to the crystal planes of ZnO (100), ZnO (002), ZnO (101), ZnO (102), and ZnO (110), respectively. With increasing solution molarities, the intensity of XRD peaks increases. However, the full width at half maximum (FWHM) of the XRD spectra decreases as the solution molarity increases from 10 to 40 mM, and then increases as the solution molarity further increases to 50 mM. The widest FWHMs of the XRD peaks in the highest-molarity ZnO nanostructures imply that this sample has a lower crystalline quality than the other samples. With high solution molarity during hydrothermal process, the growth rate may proceed too fast for regular morphology and enhance the degree of the overall nanocrystallite size fluctuation, inducing broadened FWHMs of XRD spectra [8].

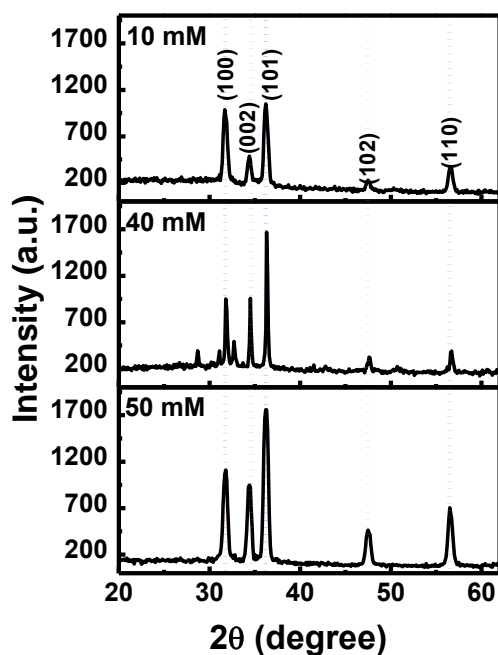


Figure 1. High-resolution X-ray diffraction spectra for the hydrothermally grown ZnO nanostructures with solution molarity 10, 40 and 50 mM, respectively.

Figure 2 shows the PL spectra of the ZnO nanostructures synthesized using different solution molarities at $T=300$ K. The ZnO nanostructures exhibit weak emission in the ultraviolet (UV) region at approximately ~ 3.2 eV (see inset of Figure 2) and a strong and broad yellow-orange emission peak at ~ 2.02 eV. The ultraviolet emission is attributed to free-exciton recombination corresponding to the near-band-edge transition in ZnO [9]. The origin of the emission peak in the visible region is related to the radial recombination of photon-generated holes with single ionized charge of the specific defects such as O vacancies or Zn interstitials [10,11]. Moreover, increasing the solution molarity from 10 to 30 mM leads to a rising of the invisible emission peak intensity. We suppose that the increase in emission intensity could be associated with the increasing concentration of the oxygen vacancies.

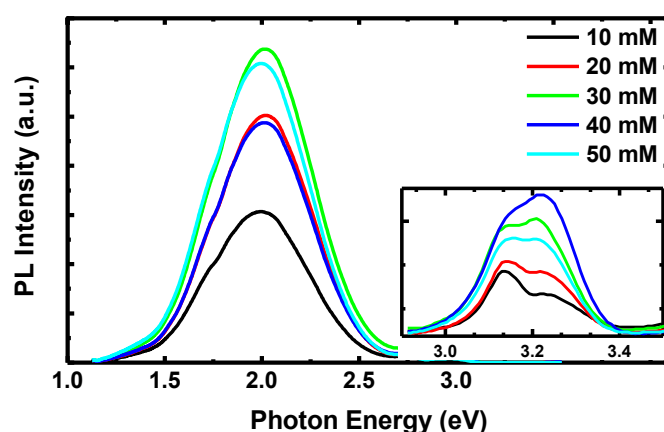


Figure 2. Room-temperature PL spectra of ZnO nanostructures with solution molarities from 10 to 50 mM. The inset shows the magnified UV emission spectral region.

More detailed data on the temperature dependence of the PL peak position and the PL linewidth taken over a broader temperature range are plotted in Figure 3. Figure 3(a) demonstrates the temperature dependent PL emission energy of ZnO sample with solution molarity 30 mM. It is apparent from the plot that the visible yellow-orange emission peaks show anomalous temperature-dependent behaviors, which differ remarkably from the monotonous band-gap shrinkage with increasing temperature. This phenomena could be associated with the defect-related levels in the ZnO nanostructures, and is attributed to the temperature related transitions between the conduction band, shallow donors (such as intrinsic Zn_i), and ionized oxygen vacancy levels [12]. The temperature-dependent FWHMs of PL spectra measured from this sample are exhibited in Figure 3(b). As temperature is increasing, the broadening of PL linewidth is obvious, resulting from the electron-phonon scattering mechanism.

Figure 4 presented the PL intensity ratio of the emission in the UV region (I_{UV}) to the emission in the visible region (I_{vis}). As comparing the optical properties of samples, the value of I_{UV}/I_{vis} of the ZnO nanostructures is an important factor [13]. It can be seen that the ratio increases as the molarity increases from 10 to 40 mM, and then decreases when the molarity further increases to 50 mM. It is known that there are more defects that could act as nonradiative recombination centers and reduce light emission on the surface compared to the internal parts of materials. The higher PL intensity ratio means fewer structural defects in the samples. Therefore, the ZnO nanostructures with molarity 40 mM have a better relative crystalline quality. Too higher solution molarity leads to the disorder of ZnO structures, and deteriorate the crystal quality.

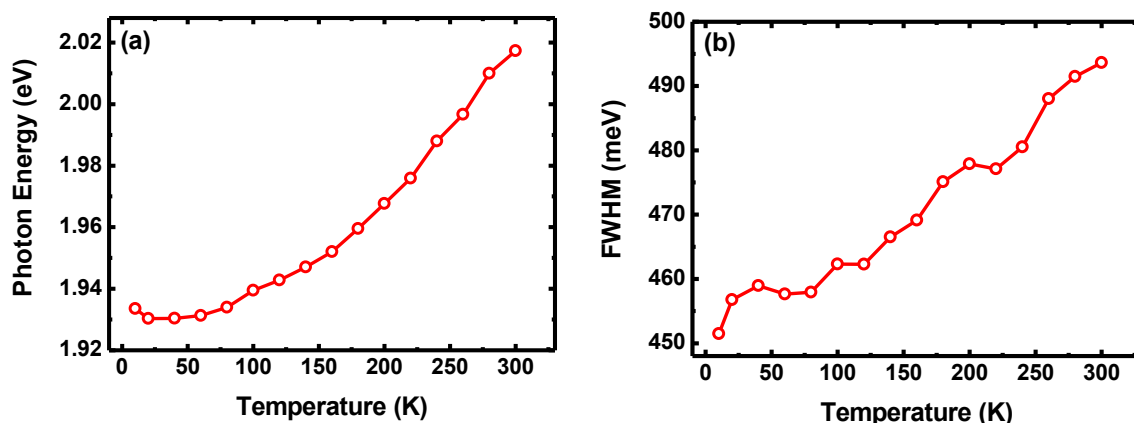


Figure 3. Temperature dependence of (a) peak position and (b) FWHM of PL spectra from the ZnO nanostructures synthesized using solution molarity 30 mM.

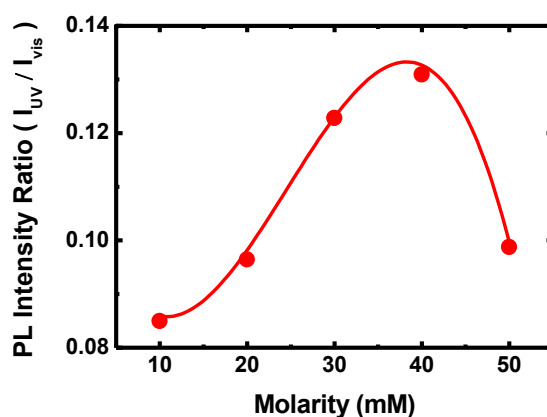


Figure 4. Variation of the PL intensity ratio of the emission in the UV region (I_{UV}) to the emission in the visible region (I_{vis}) values with various solution molarities from 10 to 50 mM.

4. Conclusions

In this paper, the effects of solution molarity on hydrothermally grown ZnO nanostructures were studied. The structural properties of the prepared ZnO nanostructures were determined by XRD measurements, and the optical properties were investigated by the measurement of temperature dependent PL spectra. It is found that the crystal quality and the optical properties are dependent on the solution molarity during hydrothermal process. The intensity of XRD peaks increase and the PL intensity ratio of the UV emission to the visible emission is also raised up with increasing solution molarities. However, the FWHM of the XRD of the ZnO nanostructures become wider and the PL emission intensity ratio (I_{UV}/I_{vis}) degrades with further increase of molarity. Therefore, the structural and optical properties of ZnO nanostructures can be improved by optimizing of solution molarity.

References

- [1] Ferro R, Rodríguez J A and Bertrand P 2008 *Thin Solid Films* **516** 2225
- [2] Rai P, Song H M, Kim Y S, Song M K, Oh P R, Yoon J M and Yu Y T 2012 *Mater. Lett.* **68** 90
- [3] Rouhi J, Alimanesh M, Dalvand R, Ooi C, Mahmud S and Mahmood M R 2014 *Ceram. Int.* **40** 11193
- [4] Jeong S H and Aydil E S 2009 *J. Cryst. Growth* **311** 4188
- [5] Willander M, Nur O, Sadaf J R, Qadir M I, Zaman S, Zainelabdin A, Bano N and Hussain I 2010 *Materials* **3** 2643

- [6] Al-lami S and Jaber H 2014 *Chem. Mater. Res.* **6** 101
- [7] Pál E, Hornok V, Oszkó A and Dékány I 2009 *Colloids Surf. A: Physicochem. Eng. Aspects* **340** 1
- [8] Zhao X, Lee J Y, Kim C R, Heo J, Shin C M, Leem J Y, Ryu H, Chang J H, Lee H C, Jung W G, Son C S, Shin B C, Lee W J, Tan S T, Zhao J and Sun X *Physica E* 2009 **41** 1423
- [9] Sui C, Lu Z and Xu T 2013 *Optical Materials* **35** 2649
- [10] Aguilar C A, Haight R, Mavrokefalos A, Korgel B A Chen S 2009 *ACS Nano* **3** 3057
- [11] Xing G Z, Yao B, Cong C X, Yang T, Xie Y P, Li B H Shen D Z 2008 *J. Alloys Compd.* **457** 36
- [12] Cao B, Cai W and Zeng H 2006 *Appl. Phys. Lett.* **88** 161101
- [13] Jayah N A, Yahaya H, Mahmood M R, Terasako T, Yasui K and Hashim A M 2015 *Nanoscale Res. Lett.* **10** 7